Petrology and geochemistry of a municipal solid waste incinerator residue treated at high temperature

Petrology and geochemistry of a municipal solid waste incinerator residue treated at high temperature

by *Daniel Traber[1]*, *Urs K. Mäder[1]* and *Urs Eggenberger[1]*

Abstract

During the 1990s, several novel high temperature processes for the treatment of municipal solid waste and its incineration residues have been developed. Residues of the VS process (Küpat AG) are examined and found to be well suited for a petrological investigation. They have basalt-like bulk compositions and consist mostly of glassy and crystalline silicates.

The CaO/SiO_2 bulk ratio is the key parameter for the behaviour on incineration. Samples with a high ratio have undergone extensive melting and formation of a matrix consisting of melilite, anorthite and a glassy to microcrystalline interstitial phase. Samples with a low ratio consist of newly formed glass with incipient crystallisation of plagioclase or of SiO_2-rich molten scrap glass. Additional observed phases include calcite, CaO, corundum, quartz, various metallic inclusions and ceramic fragments; sulphides are absent. The melilites represent solid-solutions and have a Zn content (endmember hardystonite) of about 1.5 times the bulk concentration. Plagioclase is very rich in anorthite component.

The high temperature treatment causes a significant decrease in Pb, Cd, S and inorganic carbon contents compared to conventional municipal solid waste grate-firing residues. No significant depletion in Zn and Ni is observed. Based on quantitative phase chemistry, bulk composition, and relative volumetric amount it can be shown that Zn is almost completely bound to crystalline or glassy silicates while at least 50% of the Cu is bound to metallic inclusions. Pb has been observed in minute metallic inclusions.

Keywords: Municipal solid waste incineration, melilite, waste glass, heavy metal speciation, secondary raw material.

1. Introduction

Today's municipal solid waste incinerators (MSWI) produce a very heterogeneous and reactive residue at about 850 °C (gas temperature). The only limit the combustion process has to meet to allow the residues to be landfilled according to Swiss TVA (TVA, 1990) is a maximum content of organic carbon of 3 wt%. The residues are mostly contained in landfills (there has been some use in road construction) where the leachate is collected and commonly treated in municipal sewage plants. The aqueous concentrations of most heavy metals are low due to the alkaline conditions in the leachate (JOHNSON, 1993). However, some concerns about the long-term evolution of the landfills remain because today's residues are far from being at equilibrium with respect to a hy-

drous environment, and metal speciation in the residues is rarely known. Various reactions that proceed with time reduce the alkalinity (acid neutralisation capacity) of the residues. Therefore, a decreasing pH has to be expected for the future (hundreds to thousands of years), and hence higher heavy metal concentrations in future leachates cannot completely be excluded (e.g. STÄUBLI, 1992).

Incinerating waste at higher temperature has several advantages such as homogenisation and surface area reduction by extensive melting and separation of heavy metals (by evaporation or metal-liquid separation). Material properties of the resulting residue are easier to characterise due to better homogeneity, and the residues may have a potential as secondary raw material.

In Switzerland, today's legislation prescribes bulk chemical analyses and short-term (e.g., 48 h)

[1] Rock-Water Interaction Group, Institute of Geological Sciences, Baltzerstrasse 1, CH-3012 Bern, Switzerland. <traber@geo.unibe.ch>

leaching tests for (e.g.) the classification as so-called "inert material" (TVA, 1990). However, these tests provide only little information about the possible long-term behaviour of the residue in the hydrosphere or in a construction material. The aim of our project is to understand the leaching behaviour of such high temperature residues based on detailed material characterisation combined with leaching experiments running over periods of months and geochemical modelling using computer codes for rock-water interaction. Additionally, a comparison to the weathering behaviour of natural materials will allow to identify major processes that have to be expected on a long time scale. Detailed knowledge of the residues also leads to an improved understanding of the thermal process. ZELTNER and LICHTEN-STEIGER (2001) discuss the use of petrologic methods in the design of smelting processes in the context of resource management.

This paper presents a detailed characterisation of the residues of the so called VS Kombi Reactor (Küpat AG) that are quite unique and very interesting from a mineralogical point of view. VS stands for "Verschwelen" (to smoulder) and "Schmelzen" (to melt). The investigation of these residues is part of a larger contribution of the authors to the Swiss Priority Programme "Environment" (co-ordinated project "Waste"), supported by the Swiss National Science Foundation. For further information see BRANDL et al. (1999) or TRABER (2000).

2. Sample Material and Methods

The VS process combines standard grate firing with a rotary kiln, where the final burn-out takes place and where gas temperatures of 1200 to 1400 °C are reached by guiding flammable gases generated on the grate through the kiln (without use of additional fuel). Residence times in the rotary kiln are in the range of 30 to 60 minutes. Additional information on the process can be found in KÜNSTLER et al. (1994a, 1994b) and BIOLLAZ et al. (1999).

For the present study 8 samples from test runs at the municipal solid waste incinerator (KVA) in Basel from the years 1991, 1992 and 1994 have been investigated in detail. Some samples have been studied based on several thin sections. In some charges fly ash had been added to the waste before entering the reactor. Thereby, the samples cover a wide range of input compositions and likely also different process parameters, e.g. temperature, residence time, $p(O_2)$. Considering also the better homogeneity of the Küpat samples

compared to residues from conventional grate firing, the present data-set is believed to cover the most relevant variations of the Küpat residues.

Polished thin sections of resin-embedded slag samples were used for examination by optical microscopy in transmitted and reflected light. Carbon-coated thin sections were used for investigations with a CamScan scanning electron microscope (SEM) equipped with an energy dispersive spectrometer (EDS), and for quantitative analysis with a Cameca SX-50 electron microprobe (EMP). Another part of the sample material was pulverised in a tungsten carbide mill after removal of large metal pieces (> about 1 cm) and used for quantitative bulk-chemical analysis by X-ray fluorescence analysis (XRF), to identify crystalline phases using X-ray diffraction (XRD), to determine Cd and Pb contents by acid digestion and atomic absorption spectroscopy (AAS), and for the coulometrical determination of C and S (by IR-absorption in N_2 or O_2 carrier gas).

3. Results

3.1. MACROSCOPIC AND MICROSCOPIC DESCRIPTION

The samples consist of dark porous massive slag (Fig. 1) or of only weakly bound sintered slag material (Fig. 2). All samples include macroscopically visible refractory inclusions such as scrap metal, ceramic fragments and scrap glass.

The massive slags have a crystalline matrix consisting of acicular plagioclase, tabular melilite and a glassy to microcrystalline interstitial phase (Fig. 3). The analysis of backscattered electron images yields the approximate relative ratio of 30% plagioclase, 45% melilite and about 25% interstitial phase. Plagioclase crystals display twinning and have a typical size of 10×60 μm, melilites are typically 15×30 μm. The interstitial phase, representing the residual melt after crystallisation of plagioclase and melilite, includes feathery crystals too small to be identified by SEM.

The matrix of the typically only weakly bound, sintered samples consists of newly formed glass with incipient crystallisation of plagioclase or of SiO_2-rich molten scrap glass. In the newly formed glass phase flow banding resulting from inclusions of small dark particles is visible.

All samples contain refractory, often strongly fractured quartz grains (as confirmed by XRD). Obviously these grains survived the high temperature treatment as metastable ß-quartz and were not transformed to tridymite. Other relics are strongly corroded carbonates and the dissociation
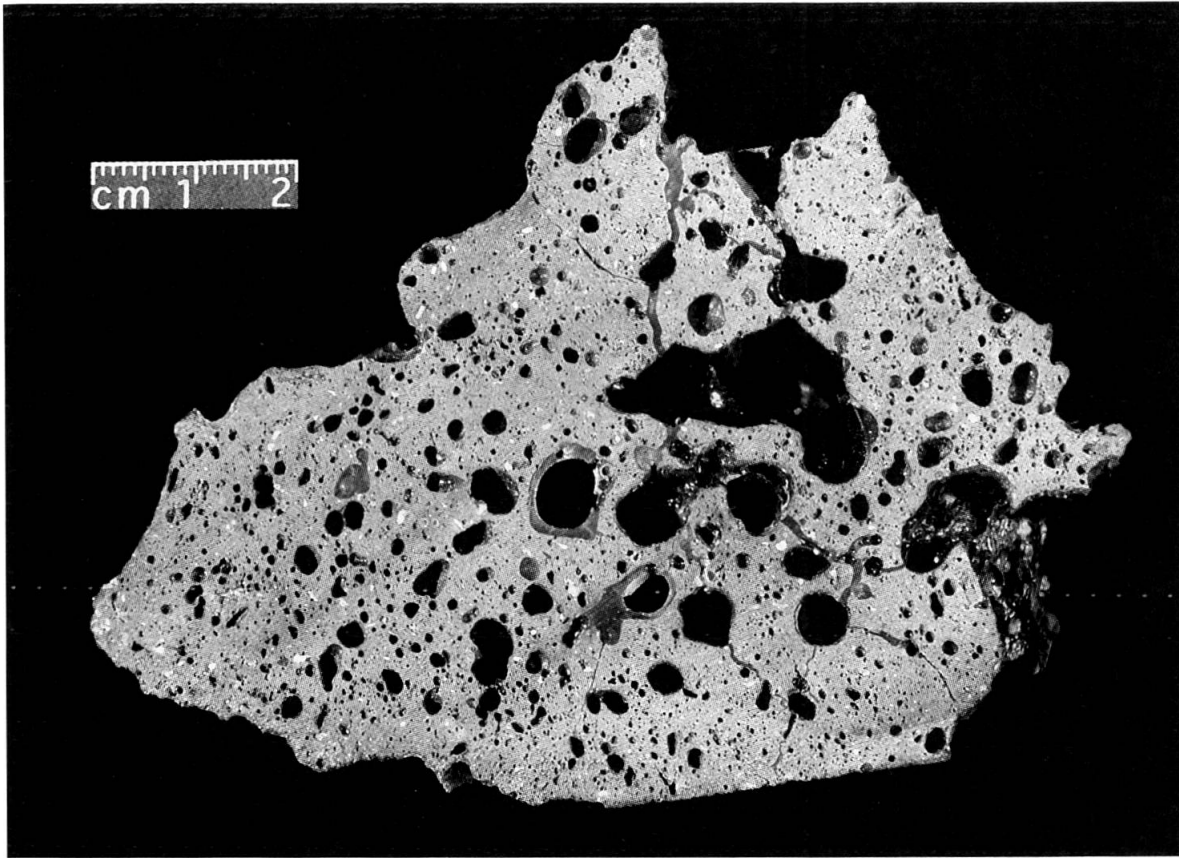
Fig. 11   Hand specimen of a relatively homogeneous massive porous slag (sample Kü2). Pores are partly filled with resin. Scale bar in [cm].
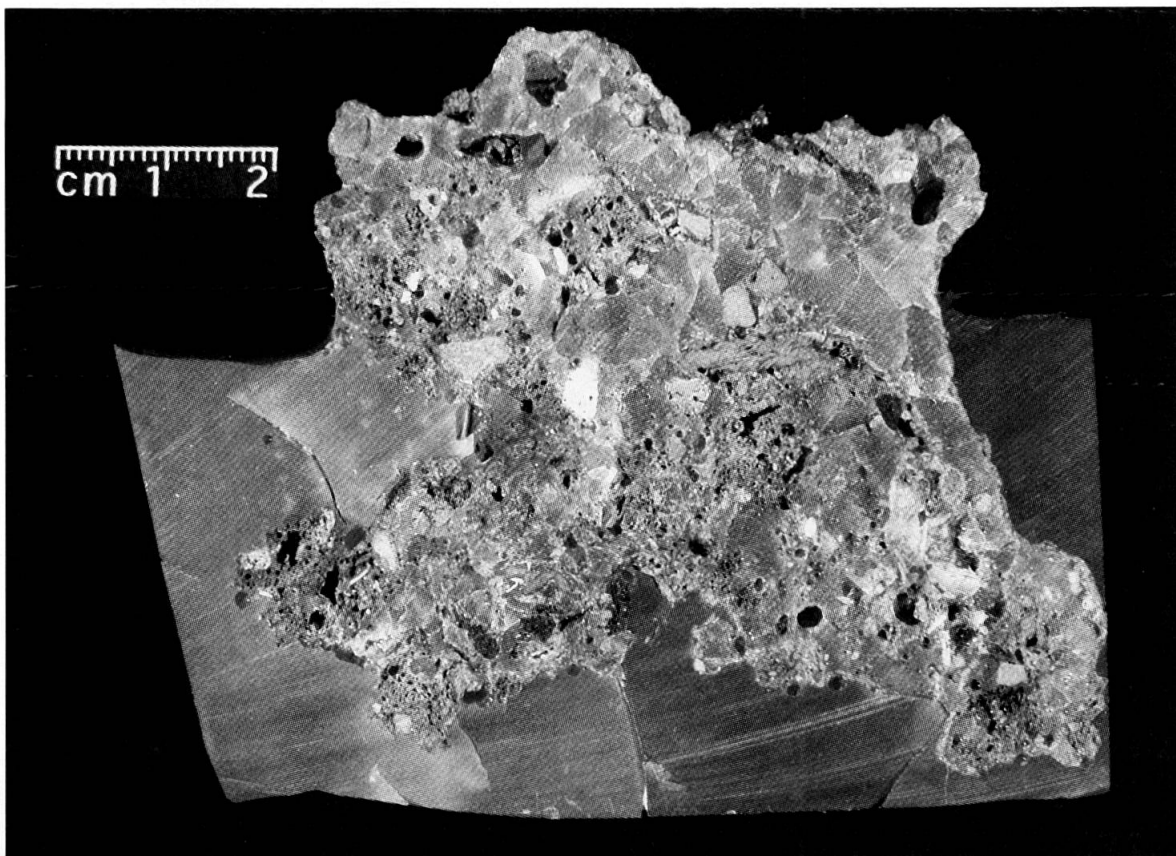

Fig. 22   Hand specimen of a heterogeneous slag embedded in resin (sample Kü6). Matrix consisting of newly formed glasss and of scrap glass with various refractory inclusions. Scale bar in [cm].
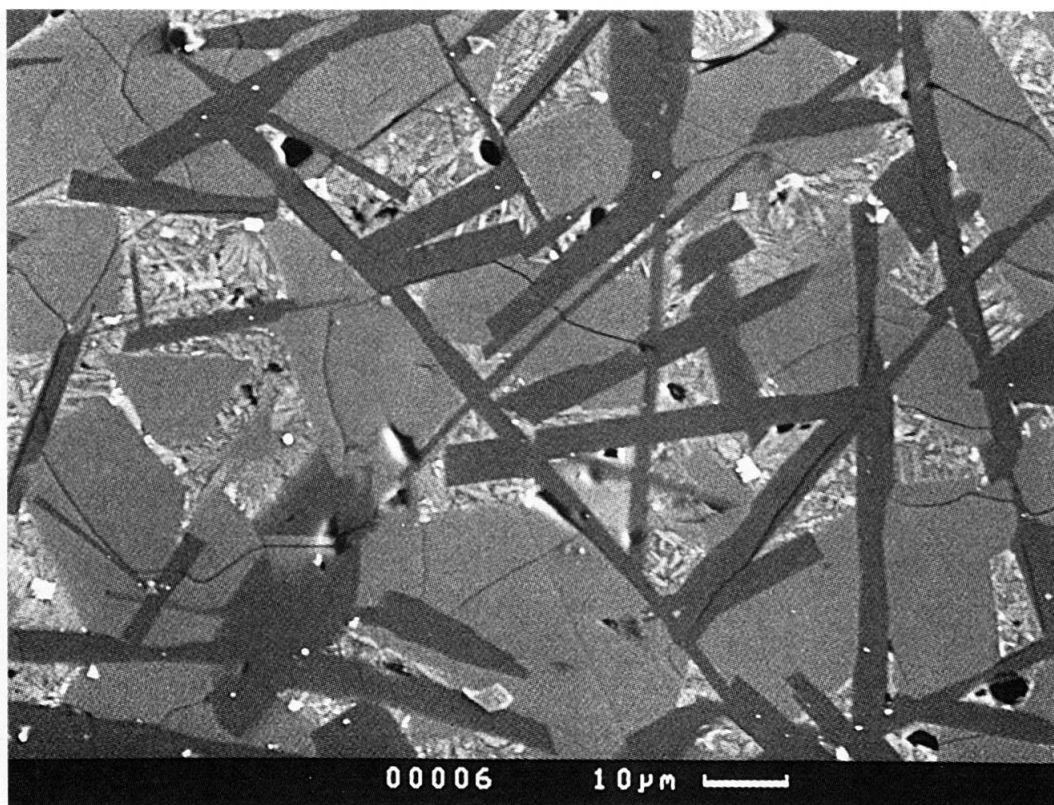
Fig. 3 Backscattered electron image of the matrix of sample Kü1. Dark needles: plagioclase, in grey: melilite and a bright microcrystalline to glassy interstitial phase. Some very small spherical metallic inclusions are visible as bright specks. Scale bar is 10 μm.

product CaO. During preparation of the thin sections CaO partly reacted with water resulting in crystal growth (portlandite or calcite) out of the thin section plane. However, in contrast to what was expected from the claimed process temperatures and from the dissociation temperature of pure calcite (894 °C at 1 atm, in air; DEER et al., 1992), some carbonate is still present. From textural obeservations, it is obvious that this carbonate survived the high temperature process and did not form during cooling.

Additional observed phases include corundum and various metallic inclusions. The latter amount to less than 1 vol% (apart from the removed large pieces of scrap iron) and comprise pure metals, alloys and metal-phosphor compounds. Metallic inclusions are preferably situated very close to gas pores. Common are Fe–P alloy inclusions, and in some cases exsolution into a Fe- and a Fe–P phase has been observed. However, pure iron is rarely observed at the thin section scale. Copper can be found pure or in alloys together with Sn, Sb and Al. Pure Al and Si are frequently observed; pure Al occurs at relatively high concentrations in the glassy samples. Zinc is detected in minor concentration in alloys with Al and Si. Lead is observed in the form of minute

metallic spheres. No phase containing Cd could be detected with the analytical tools available. Sulphides are absent.

The loss on ignition determined at 1050 °C is the result of the loss of volatile compounds (e.g. CO_2) and of weight gained by oxidation (negative values). The average loss on ignition of 8 samples is –0.3%, with a maximum of +0.4 and a minimum of –1.0%. For comparison, the average loss on ignition of residues of conventional grate firing incinerators determined at 550 °C amounts to 3.5 wt% (n = 11, σ_{n-1} = 0.6 wt%; calculated using data from GANGUIN, 1998).

3.2. BULK CHEMICAL COMPOSITION

Results of the bulk chemical analysis of major and trace elements are given in Table 1. The average of 11 analyses from 3 different conventional Bernese incineration plants, calculated from data published by GANGUIN (1998), is indicated for comparison. The exact composition of the waste input into the VS Kombi reactor is unknown. Bulk slag composition is not only a function of the incineration process, but depends to a large extent on the input material, which varies with area

Table 1 Bulk chemical composition of samples Kü1 to Kü8 compared to an average reference slag (see text). Fly ash containing samples are marked with a +. Cryst. – Crystalline type sample. stdev. – standard deviation (σ_{n-1}), n. a. – not analysed.

Sample	Kü1	Kü2	Kü3	Kü4	Kü5	Kü6	Kü7	Kü8	average	Ref.-	slag
Fly ash	–	–	+	+	–	+	+	+			stdev
Type	Cryst.	Cryst.	Cryst.	Cryst.	Glassy	Glassy	Glassy	Glassy			
Major elements [wt%]											
SiO$_2$	38.5	38.9	38.7	40.2	48.6	48.7	43.3	42.2	42.4	44.7	4.2
TiO$_2$	2.3	2.1	2.2	1.9	1.9	1.6	2.2	2.0	2.0	1.4	0.2
Al$_2$O$_3$	21.9	20.7	20.8	22.1	19.1	17.1	21.0	21.0	20.5	13.8	2.8
FeO tot	3.1	3.3	3.5	3.7	2.6	2.4	2.9	2.9	3.04	8.4	2.4
MgO	3.4	3.6	3.7	3.6	4.4	3.4	3.7	3.8	3.7	3.0	0.4
CaO	25.3	24.9	24.8	21.8	15.2	18.4	21.0	21.8	21.6	18.9	2.2
Na$_2$O	1.9	2.1	2.0	2.4	2.1	4.5	2.4	2.4	2.5	3.6	0.5
K$_2$O	0.8	1.1	1.1	1.4	1.6	1.4	1.4	1.4	1.3	1.7	1.0
P$_2$O$_5$	1.6	1.6	1.6	1.5	1.3	1.3	1.5	1.8	1.5	1.2	0.2
Trace elements [ppm]											
Ba	3130	2683	2779	2832	2237	1943	2800	2119	2565	2085	1263
C inorg	1300	1300	2800	1700	800	4700	1100	8600	2788	7260	1640
Cr	663	516	537	517	439	438	540	637	536	1469	2120
Cu	847	1021	833	1160	946	1099	810	864	947	2392	944
Cd	1.5	0.7	0.7	0.1	0.1	0.2	0.1	n.a.	0.5	5.7	5.1
Mn	1084	929	929	774	542	542	620	620	755	930	77
Ni	158	105	101	63	91	85	80	113	99	192	145
Pb	164	165	148	112	70	284	85	202	154	1824	965
S	200	300	200	300	300	600	500	n.a.	343	3200	1500
Sr	367	349	356	328	291	250	305	307	319	301	76
V	41	44	42	43	44	40	42	56	44	39	11
Zn	7515	4761	4033	2016	506	1022	523	662	2630	4285	1830
Zr	198	189	190	180	165	167	173	169	179	426	585
Total	100.3	99.5	99.6	99.5	97.4	99.8	100.0	100.2	99.5	99.2	–

(urban vs. countryside), season and waste management policies (e.g. separate collection of compost, PET etc.).

80 wt% of the bulk composition of the samples can formally be accounted for by the oxides of Al, Ca and Si. While the Al content is relatively constant, the CaO/SiO$_2$ ratio (weight) varies between 0.3 and 0.7. Compared to the reference slags the samples are Al-rich and Fe-poor. The elevated Al contents in the high temperature residues may result from increased melting, oxidation of scrap Al, and incorporation of Al$_2$O$_3$ into the silicate melt (resulting in less Al scrap being removed during sample preparation). The differences in Fe content may point to different efficiencies in the removal of scrap metal.

Trace element contents show variations of up to about one order of magnitude. The fly ash containing samples do not show a characteristic composition compared to the samples free of fly ash: The amount of fly ash added must have been small compared to the chemical variation of the input material and/or volatile elements contained in fly ash have apparently re-evaporated. The average contents of inorganic carbon, S, Cu, Cd,

Ni, Pb, and Zn (Fig. 4) are lower than in the reference material, but the differences in Ni and Zn contents are not significant based on a 95% confidence interval. The average Cu content is about 40% of the reference slag, while the Pb and Cd relative contents amount to about 10%.

The high temperature process decreases the average S contents to about 10% and of the inorganic carbon content to about 40% of the reference slag. It is expected that the Küpat process also causes a significant decrease of organic carbon content compared to a conventional grate firing process because of the high temperature treatment under oxidizing conditions and the agitation of the waste in the rotary kiln. However, the organic carbon content was analysed in sample Kü8 only (the sample with the highest inorganic carbon content): The analysis yielded 0.49 wt%, which corresponds to 36% of the average value of the reference samples (average 1.37 wt%, n = 11, σ_{n-1} = 0.71 wt%). These observations are supported by the low weight changes on ignition of the Küpat samples compared to conventional grate firing residues.

While all analyses of Cd, Pb and Ni are below the current limits for disposal of inert materials defined in the Swiss TVA ("Technische Verordnung über Abfälle"; TVA, 1990), all Cu and 5 out of 8 Zn contents are above these values. The good performance with respect to the concentration limit of Pb is likely due to the high temperature process (Fig. 4).

Empirically one observes lower concentrations of FeO and higher concentrations of Na_2O and K_2O in the glassy samples than in crystalline ones. While Fe^{2+} is considered a network-breaking element in silicate liquids, Fe^{3+} is considered a network former. Ferrous iron may thus further reduce the viscosity in the samples with high CaO/SiO_2 ratio and thereby facilitate crystallisation processes. However, Na and K are also network-breaking elements and they appear to be enriched in the glassy samples.

Although it is obvious from the microscopic investigation that the melt was never homogeneous, projection of the bulk composition into the melt system Al_2O_3–CaO–SiO_2 (Fig. 5) provides important information on the crystallisation sequence. All compositions plot in the primary field of anorthite (An); crystalline samples containing melilite plot closer to the cotectic line with gehlenite. The CaO/SiO_2 ratio (weight) is of fundamental importance in the formation of melilite. Glassy samples have a ratio below 0.52, crystalline samples a ratio above 0.54. However, this simplified melt system cannot explain satisfactorily the formation of the complex melilites. Extending the system to 5 wt% MgO, and hence allowing for the formation of åkermanite component (Mg-melilite), moves the stability field of melilite from a minimum CaO/SiO_2 ratio of 0.92 to about 0.74 (EISENHÜTTENLEUTE, 1995, p. 160). In this system, anorthite is expected to form as a primary phase in the samples in the temperature range of about 1300 to 1400 °C, followed by simultaneous crystallisation of anorthite and melilite. Taking Na into account lowers the liquidus temperatures additionally.
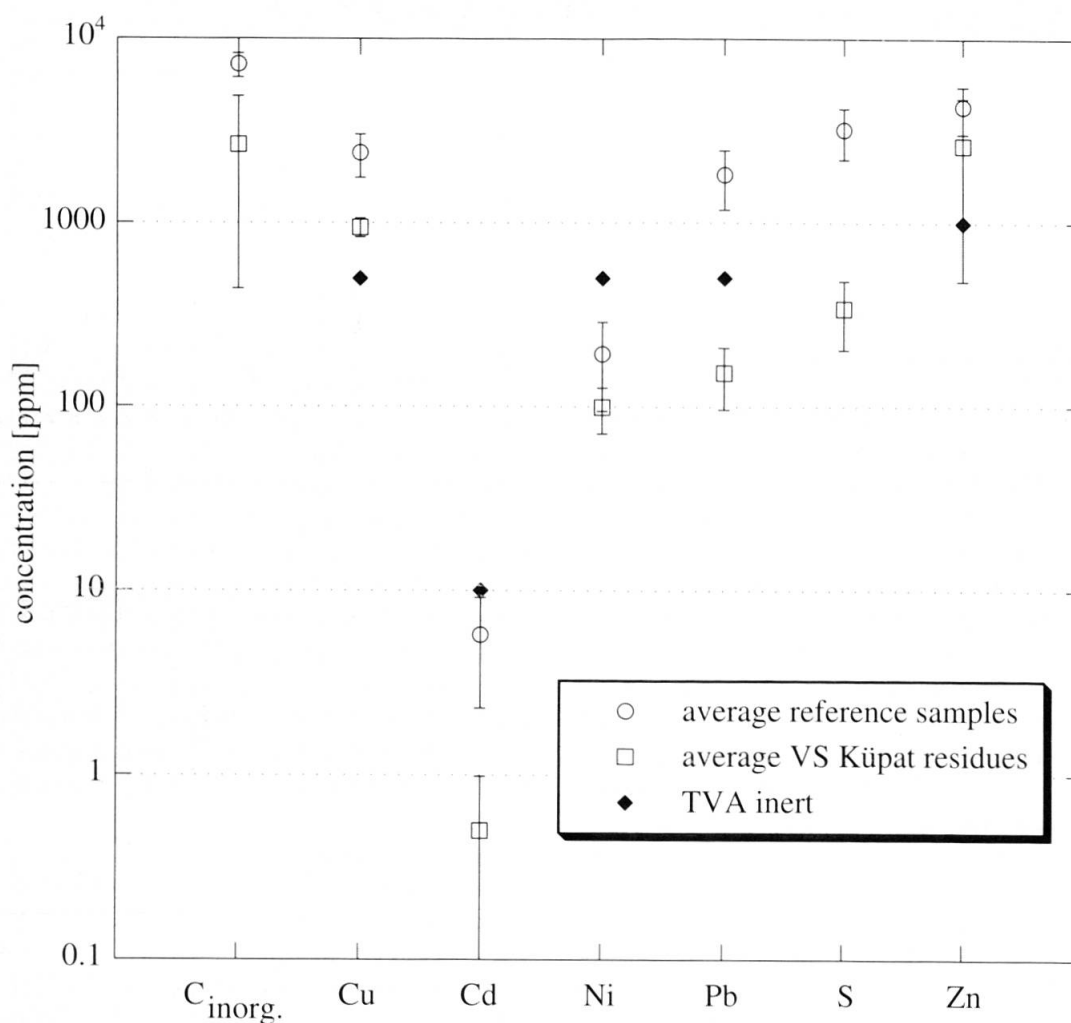

Fig. 4 Average contents of heavy metals, S and inorganic C compared to values of a conventional MSWI residue and to limits defined for inert materials according to Swiss TVA. The range defined by the error bars represents a 95% confidence interval.

Modelling melt viscosities of a sample with high (Kü1) and low (Kü6) CaO/SiO_2 ratio using the model of SHAW (1972) yields differences in melt viscosity of 1 to 1.5 log units in the temperature range of 1200 to 1400 °C.

3.3. QUANTITATIVE PHASE CHEMISTRY

Plagioclase: The plagioclase crystals are very rich in An component (Table 2). With the exception of sample Kü4, An-contents are above 90 mol%, Ab-contents are about 5%, and the K- and Ba-feldspar contents are typically below 1%. Comparison of plagioclase composition within a sample yields only slight differences, e.g. the standard deviation for CaO calculated from analyses of different plagioclase crystals within a sample is about 3%. The chemical analyses yield only small amounts of impurities such as Fe, Mg, P, Ti and Zn. Concentrations of the routinely analysed elements Cl, Cr, Cu, Mn, Pb and S are below de-

tection limits (0.01 to 0.05 wt%). The small grain size of plagioclase crystals in sample Kü4 likely explains the larger deviation to expected feldspar stoichiometry.

Melilite: The melilite family comprises the endmembers gehlenite (Gh, $Ca_2[Al_2SiO_7]$), åkermanite (Ak, $Ca_2[MgSi_2O_7]$), Na-melilite (NaCa[AlSi$_2O_7$]), Fe-åkermanite (Fe-Ak, $Ca_2[Fe^{2+}Si_2O_7]$), Fe-gehlenite (Fe-Gh, $Ca_2[Fe^{3+}AlSiO_7]$) and hardystonite ($Ca_2[ZnSi_2O_7]$). Melting points of the endmembers as well as liquidus and solidus temperatures of the binary solid solutions are well known (e.g., DEER et al., 1962, 1986). Addition of Na significantly lowers the crystallisation temperatures: In the system Gh - Na-melilite, for example, from about 1600 °C of pure Gh to 1185 °C at 95 mol% Na-melilite (DEER et al., 1962). Liquidus temperatures for the system Gh - Ak - Na-melilite are published in LEVIN et al. (1969): With decreasing temperature melilite compositions are directed towards the Na endmember (Fig. 6). Our own melting experiments on the Küpat samples
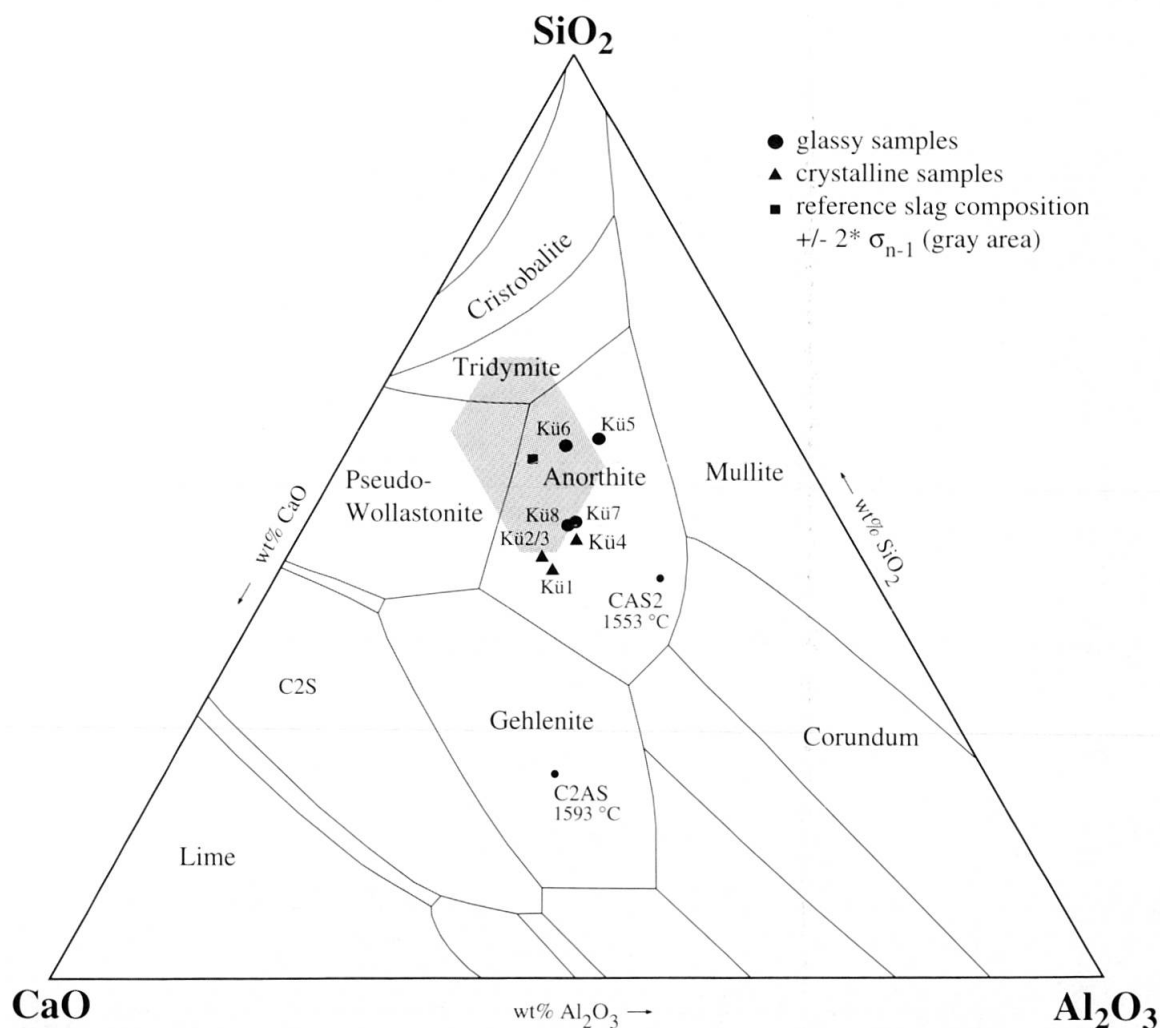

Fig. 5 Projection of bulk compositions into the melt system CaO–Al_2O_3–SiO_2 (redrawn form LEVIN, 1964) and comparison to reference bottom ash (grey area).

indicate a liquidus temperature for these complex melilites (see below) of about 1200 °C.

Melilite compositions within a sample show larger variations than comparing average compositions of different samples. The average melilite consists of about 30 mol% Gh, 37% Ak, 23% Na-melilite, 5% Fe-Ak and up to 5% hardystonite component. The compositional range of melilites of sample Kü1 is listed in Table 3 and plotted in Fig. 6. The endmember calculations assumed all iron to be incorporated into Fe-Ak.

Zn concentrations in melilite were found to be linearly correlated with bulk Zn contents (Fig. 7): The Zn contents in melilites are 1.5 times the residue bulk composition. The linear regression equation of average melilite Zn content as a function of bulk content (based on data from 4 samples and 6 thin sections) is:

$$ZnO_{mel} = 1.45 \times ZnO_{bulk} + 0.2 \quad (R^2=0.95).$$

Empirically one observes a trend towards lower ZnO concentrations in melilite with increasing Na-melilite component. This might indicate that Zn partitioning into melilite is more marked at higher temperatures. This observation could be of importance for Zn partitioning in melts of conventional MSWI, where melilite has also been reported (no quantitative analyses are known so far).

The contents of BaO (<0.08 wt%), Cl (<0.02), Cr_2O_3 (<0.01), CuO (<0.04), PbO (<0.05) and SO_3 (<0.02) in the analysed melilites were below the detection limits.

Table 2 Average plagioclase compositions from n microprobe analyses Total of cations normalised to 5. Ab: Albite, An: Anorthite, Or: Orthoclase, Cel: Celsian. Numbers of major elements should be considered precise to one decimal place only.

| Sample	Kü1	Kü2	Kü3	Kü4	Kü7
n	9	7	7	6	3
SiO_2	44.03	44.32	44.41	45.25	44.91
TiO_2	0.18	0.22	0.22	0.49	0.34
Al_2O_3	35.38	34.96	35.17	32.58	35.58
FeO tot	0.11	0.17	0.22	0.43	0.17
ZnO	0.06	0.06	<0.05	0.06	<0.05
MgO	0.12	0.21	0.19	0.63	0.14
CaO	19.50	19.58	19.31	18.80	18.99
BaO	0.15	0.26	0.28	0.23	0.35
Na_2O	0.48	0.57	0.64	1.04	0.61
K_2O	0.10	0.13	0.15	0.33	0.13
P_2O_5	0.05	0.08	0.13	0.41	0.10
Total [wt%]	100.17	100.55	100.72	100.26	101.31
Si	2.033	2.040	2.038	2.086	2.053
Ti	0.006	0.008	0.008	0.017	0.012
Al	1.926	1.896	1.903	1.770	1.917
Fe	0.004	0.007	0.008	0.017	0.006
Zn	0.002	0.002	–	0.002	–
Mg	0.008	0.014	0.013	0.043	0.009
Ca	0.965	0.966	0.949	0.929	0.930
Ba	0.003	0.005	0.005	0.004	0.006
Na	0.043	0.051	0.057	0.093	0.054
K	0.006	0.008	0.009	0.019	0.008
P	0.002	0.003	0.005	0.016	0.004
Total cations	5.000	5.000	5.000	5.000	5.000
Σ(Ca,Na,K,Ba)	1.017	1.028	1.021	1.045	0.998
Σ(Al,Si,Fe,Ti,Mg)	3.978	3.965	3.970	3.934	3.997
Ab [%]	4.3	4.9	5.6	8.9	5.4
An [%]	94.9	93.9	93.0	88.9	93.2
Or [%]	0.6	0.7	0.9	1.9	0.8
Cel [%]	0.3	0.5	0.5	0.4	0.6
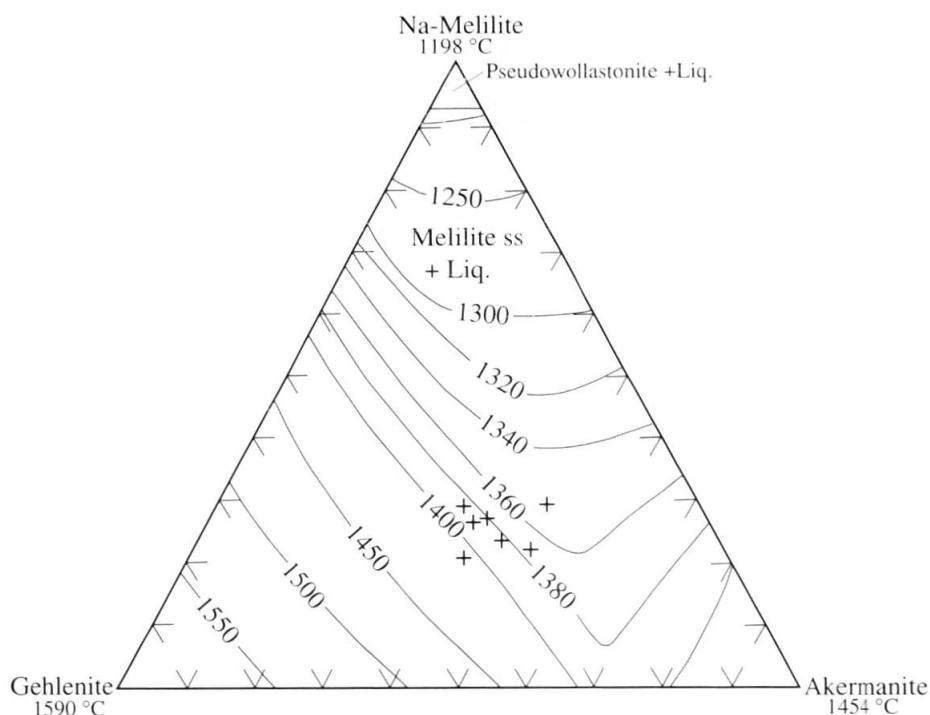
Fig. 6 Projection of melilite compositions of sample Kü1 (Table 3) into the melt system Na-melilite–gehlenite–åkermanite. Redrawn from LEVIN et al. (1969, Fig. 2690).

Table 3 Microprobe analyses of melilites in sample Kü1. Total of cations normalised to 5. The endmember calculations assumed all iron to be incorporated into Fe-Ak. Numbers of major elements should be considered precise to one decimal place only.

| Analysis no.	1	2	3	4	5	6	7	8
SiO_2	39.53	39.81	38.61	38.17	37.74	37.42	36.43	36.55
TiO_2	0.19	0.15	0.12	0.14	0.11	0.09	0.12	0.06
Al_2O_3	12.31	12.38	13.03	14.29	15.58	16.36	16.67	16.39
FeO tot.	1.37	1.4	1.38	1.28	1.12	1.12	0.91	1.12
MnO	0.06	0.06	0.06	0.03	0.03	0.06	<0.01	0.08
ZnO	1.54	1.57	1.63	1.45	1.47	1.39	1.32	1.50
MgO	6.34	6.43	6.29	5.93	5.43	5.21	4.85	5.44
CaO	35.57	35.68	36.37	36.5	35.98	36.13	35.66	36.72
Na_2O	2.97	2.95	2.34	2.32	2.81	2.75	3.03	2.24
K_2O	0.14	0.14	0.15	0.13	0.14	0.13	0.13	0.13
P_2O_5	0.15	0.17	0.05	0.04	0.18	0.08	0.27	0.05
Total [wt%]	100.16	100.74	100.03	100.28	100.59	100.75	99.41	100.28
stoichiometry:								
Si	1.795	1.797	1.762	1.736	1.705	1.688	1.662	1.661
Ti	0.006	0.005	0.004	0.005	0.004	0.003	0.004	0.002
Al	0.659	0.659	0.701	0.766	0.830	0.870	0.896	0.878
Fe	0.052	0.053	0.053	0.049	0.042	0.042	0.035	0.043
Mn	0.002	0.002	0.002	0.001	0.001	0.002	0.000	0.003
Zn	0.052	0.052	0.055	0.049	0.049	0.046	0.044	0.050
Mg	0.429	0.433	0.428	0.402	0.366	0.350	0.330	0.369
Ca	1.730	1.726	1.778	1.779	1.742	1.746	1.743	1.788
Na	0.261	0.258	0.207	0.205	0.246	0.241	0.268	0.197
K	0.008	0.008	0.009	0.008	0.008	0.007	0.008	0.008
P	0.006	0.006	0.002	0.002	0.007	0.003	0.010	0.002
Total cations	5.000	5.000	5.000	5.000	5.000	5.000	5.000	5.000
Endmembers [%]:								
Gehlenite	19.9	20.0	24.7	28.1	29.2	31.5	31.4	34.0
Åkermanite	42.9	43.3	42.8	40.2	36.6	35.0	33.0	36.9
Na-Melilite	26.1	25.8	20.7	20.5	24.6	24.1	26.8	19.7
Fe-Åkermanite	5.2	5.3	5.3	4.9	4.2	4.2	3.5	4.3
Hardystonite	5.2	5.2	5.5	4.9	4.9	4.6	4.4	5.0
	99.3	99.6	99.0	98.5	99.5	99.4	99.1	99.9
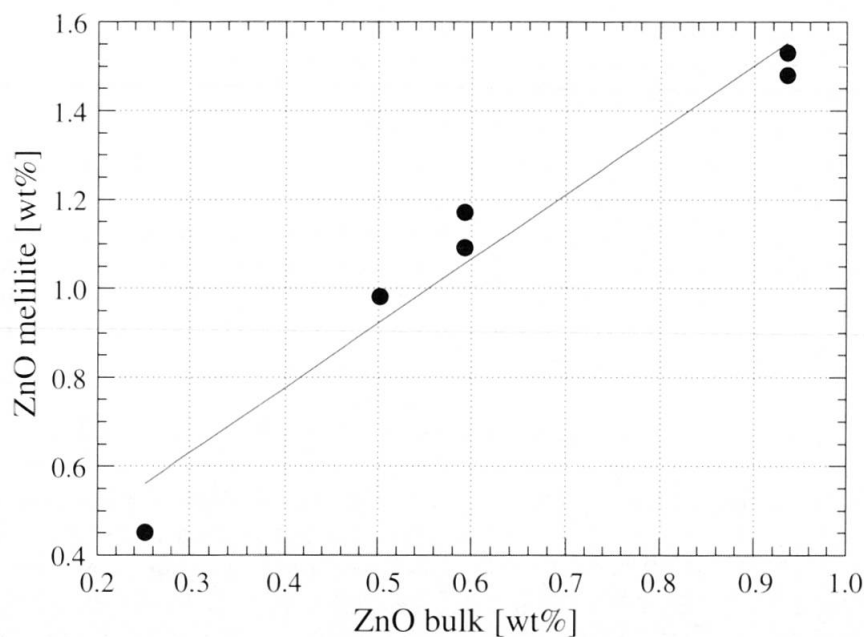
Fig. 7 Bulk ZnO concentration versus average ZnO concentrations in melilite. The linear regression equation is $ZnO_{mel} = 1.45 \times ZnO_{bulk} + 0.2$ ($R^2 = 0.95$). Analyses from 6 thin sections of 4 different samples.

Table 4 Average compositions from n microprobe analyses [wt%] of the interstitial phase (inter) of samples Kü1 to Kü4 and of the glass phase of samples Kü5 to Kü7. Numbers of major elements should be considered precise to one decimal place only.

sample phase n	Kü1 inter 17	Kü2 inter 11	Kü3 inter 8	Kü4 inter 24	Kü5 glass 16	Kü6 glass 7	Kü7 glass 18
SiO_2	36.53	37.47	40.19	40.91	52.58	79.55	41.79
TiO_2	5.08	3.16	2.02	2.32	2.13	0.05	2.54
Al_2O_3	16.29	13.11	27.06	19.48	14.89	1.64	20.30
Cr_2O_3	0.05	0.02	0.05	0.10	0.08	0.03	0.10
FeO tot	5.28	4.02	2.00	2.64	1.50	0.12	1.10
MnO	0.29	0.19	0.10	0.12	0.09	<0.02	0.08
CuO	<0.04	<0.04	<0.04	<0.04	<0.04	<0.04	<0.04
ZnO	0.76	0.75	0.20	0.25	0.06	<0.05	0.07
MgO	3.32	4.36	1.40	4.12	4.47	2.68	3.96
CaO	23.49	29.16	22.70	24.29	17.81	9.85	24.56
BaO	0.62	0.44	0.56	0.39	0.24	<0.08	0.18
PbO	<0.05	<0.05	<0.05	<0.05	<0.05	<0.05	<0.05
Na_2O	2.13	2.43	1.08	2.27	2.56	6.25	2.43
K_2O	2.30	1.98	1.01	1.65	2.19	0.76	1.51
P_2O_5	3.83	3.18	1.74	1.74	1.19	0.02	1.47
SO_3	0.19	0.12	0.08	0.08	0.09	0.16	0.17
Cl	0.14	0.11	0.06	0.08	0.10	0.03	0.12
Total	100.34	100.62	100.28	100.49	99.98	101.14	100.38

Interstitial phase: Compared to plagioclase and melilite this phase is enriched in the elements K, Fe, Cl, S, Ba, P, Cr, Ti and Mn (Table 4). The concentrations of PbO and CuO are below the detection limits. As can be expected for a phase representing a residual melt, analysis yield large variations within a sample and relative standard deviations are in the range of x × 10%, even higher for trace elements.

Glass matrix: Average compositions of the glass matrix of samples Kü5 to Kü7 (glassy type) are listed in Table 4. The glasses are homogeneous on a thin section scale as far as major elements are concerned. While the analyses of sample Kü5 and Kü7 reflect the bulk composition, the analysis of sample Kü6 is obviously from an area of molten Ca-Na-silicate scrap glass. Note that the highest CaO/SiO_2 ratio of the glass matrix is observed in sample Kü7, the glassy sample with incipient crystallisation of plagioclase in the matrix. As in the other silicate phases, CuO and PbO concentrations were below the detection limit of the microprobe.

3.4. DISTRIBUTION OF THE ELEMENTS

From the bulk composition, phase chemistry and relative amount of each phase one can compute the relative distribution of the elements among the different phases. This is of particular interest with respect to heavy metals.

To recalculate the volume fraction into the weight fraction of a phase, density must be considered. Anorthite has a density of 2.76 g/cm³, melilite about 3.0, glasses of comparable composition to the glass phase are 2.8 to 3.0, and the bulk density of the samples is 2.77 (glassy type; JACOBS, 1998). The density of the interstitial phase is not known, but from backscattered electron images (higher than melilite) and from chemical composition it is roughly estimated to be about 3.2. This shows that all glassy and crystalline silicate phases are within 10 to 15% of the bulk density. Other phases, such as the metallic inclusions, cannot be accounted for with average compositions and densities. Additionally, the composition of the interstitial phase yielded a relatively large variation.

Due to these uncertainties the calculation of elemental distributions has been simplified in the following way: (a) For the crystalline samples it is estimated that plagioclase, melilite and interstitial phase account for 97%. The relative ratios of these phases are given in section 3.1. A phase termed "residual" is defined as the difference between bulk composition minus the amount accounted for by plagioclase, melilite and interstitial phase. This residual phase contains the metallic inclusions among others (section 3.1). Densities are neglected. (b) In the glassy samples only the glass matrix is sufficiently defined, for which an amount of 90% has been estimated. Further procedures as with the crystalline samples. No elemen-
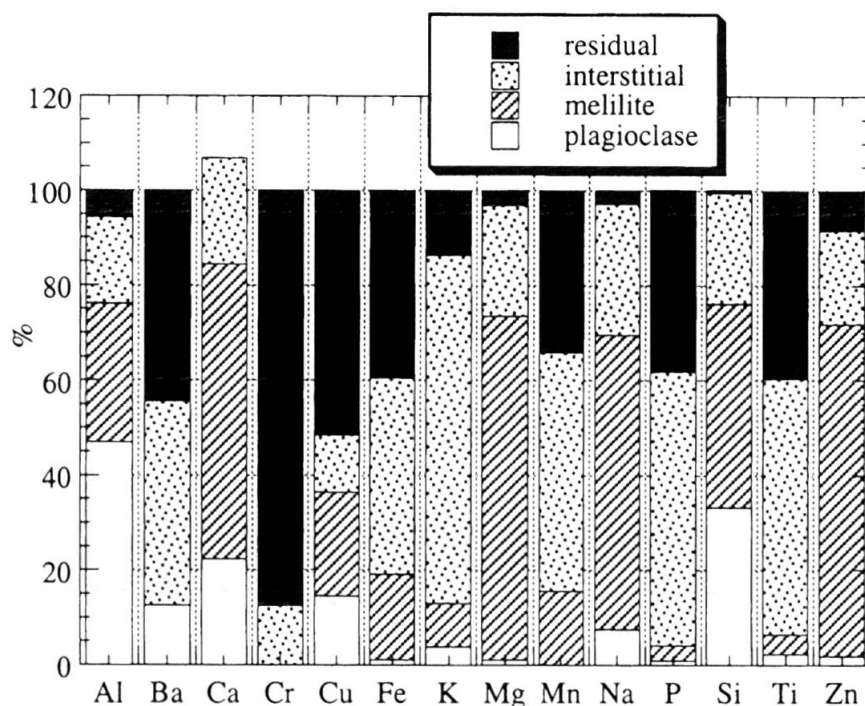
Fig. 8   Element partitioning in a crystalline type sample (Kü1). For element Cu see text.
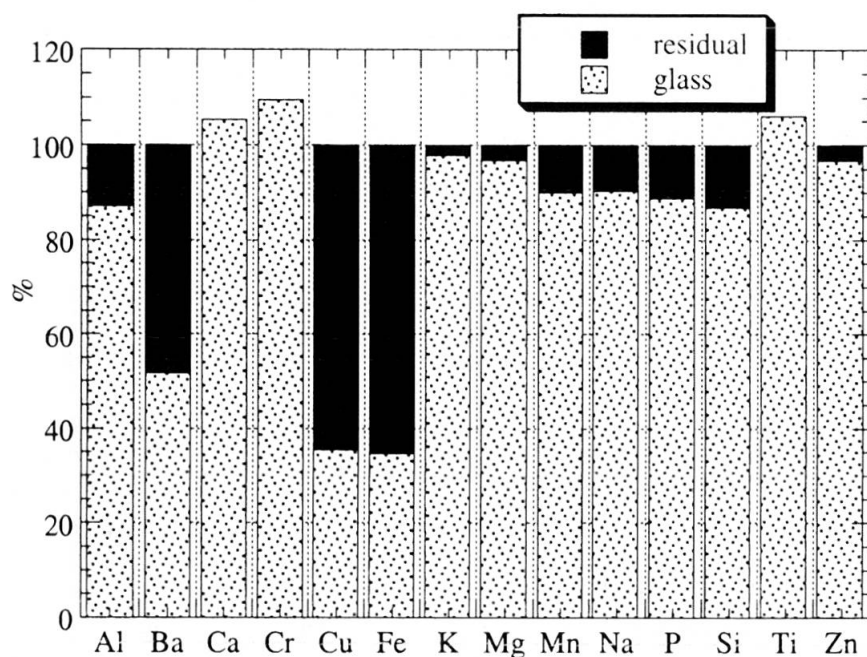

Fig. 9   Element partitioning in a glassy type sample (Kü7). For element Cu see text.

tal distribution has been calculated for sample Kü6 where the composition of the analysed glass phase is not representative of the bulk sample.

Figure 8 shows the element partitioning in a crystalline sample. Note the preferential incorporation of Zn into melilite and to a lesser extent into the other silicate phases; very little Zn remains bound to metal phases. Cu could not be detected in the silicate phases: Assumption of a concentration equal to the detection limit leads to an estimate that at least 50% of Cu is bound to metallic inclusions (likely much more). Due to the high detection limits of the microprobe relative to the bulk content no quantitative statement about Cd and Pb can be made. However, Pb has been observed to form minute metallic inclusions. The distribution of Ba cannot be explained at present. The total of Ca above 100% in this figure may be due to a volumetric overestimation of melilite (the major carrier of this element).

Figure 9 shows the element partitioning in a glassy sample. Zn is concentrated in the glass phase, while Cu is bound to at least 60% to metallic inclusions (same assumption as above). A significant amount of Al appears to be present in metallic form, in agreement with the microscopic observation (section 3.1). The elements Cr, Mn, Ti and P are obviously much easier to incorporate into the glass phase than into the above silicate phases.

4. Discussion

The samples show a close relationship between bulk composition, melting behaviour and crystallisation. Samples with high CaO/SiO_2 ratios have undergone intense melting, crystallisation of melilite and plagioclase and more extensive homogenisation than the samples with low ratios. The latter are glassy, often only sintered, with none or incipient crystallisation of plagioclase. Higher CaO/SiO_2 ratios in melts promote crystallisation because diffusion rates are higher due to lower viscosities. Additionally, melting has reduced the amount of ash fraction (in conventional incinerator slags around 45%, LICHTENSTEIGER and ZELTNER, 1993), and therefore also the specific surface area. Volatile elements under high temperature conditions such as Cd, Pb, inorganic carbon, S and likely also organic carbon are significantly depleted compared to a conventional grate firing reference slag. Zn on the other hand is known to have a high affinity for silicate melts (TRABER et al. 1999), and once it is dissolved in the melt it is no longer available for evaporation (except if the incinerator atmosphere is artificially enriched in HCl gas; WOCHELE et al., 1997). The present study confirms that the high-temperature treatment does not result in a higher fraction of Zn transferred from the slag into the fly ash. For the first time it is shown quantitatively that Zn is almost completely bound to glassy or crystalline silicate phases. The difference in Cu contents compared to the reference slag is small and likely due to the limited volality of Cu during MSWI (WOCHELE et al., 1997). In the investigated residues the relatively short residence time in the rotary kiln is likely an additional important parameter.

Municipal solid waste is very heterogeneous, and during the incineration and melting process a large variety of reactions take place, such as phase transformation and neoformation, evaporation and redox reactions. If these reactions are fast enough or if sufficient time is available, these reactions will guide the residue towards equilibrium (at the given temperature and incinerator atmosphere). The quality of the melting process and the degree of homogenisation in the residue can therefore be described by investigating the phase assemblage. The investigated samples display a wide variety of disequilibrium features. For example, melilite coexists with (refractory) quartz, and Al occurs in metallic form and bound to silicates and oxides. Redox conditions are of particular interest for heavy metal speciation. Metallic Al and Si are considered strong reducing agents in silicate melts (ZELTNER, 1998). From the redox-equilibrium point of view it is not expected that elements like Cu and Pb will be oxidised and incorporated into glassy or crystalline silicate phases as long as metallic Al and Si are present.

The maximum temperature attained during the incineration process in the waste material is difficult to estimate from the study of the products of the thermal process. Other parameters than bulk composition of the melt on incineration, such as $p(H_2O)$ are largely unknown. For example, it is known that åkermanite may form in the presence of excess H_2O from wollastonite and monticellite already at 685 °C at 1 atm (YODER, 1973). Inclusions of scrap Cu (T_{fusion} = 1083 °C) appear to be molten only partly or for a short time (textural evidence). The incomplete dissociation of $CaCO_3$ to CaO is likely strongly influenced by grain size, $p(CO_2)$, and agitation of the waste on incineration. IBERG (1971) studied the dissociation of carbonate during clay brick production: The thermal decomposition of calcite cannot be treated as a simple carbonate dissociation, but has to be discussed as a function of temperature, $p(CO_2)$, grain size, and interactions with silicates (e.g., formation of wollastonite). The dissociation in a size fraction <2 µm is reported at 700 to 750 °C and in material with about 30% silt fraction in the range of 850 to 900 °C. Additionally, due to the heterogeneity of MSW and the short residence times in the rotary kiln, local temperature variations in the material on incineration are likely to be large.

Although not every phase could be characterised in terms of average composition and relative amount, it was possible to show semi-quantitatively the distribution of the elements. While Zn is almost completely bound to glassy and crystalline silicate phases, the major part of Cu has to be expected in metallic form. While Pb has been observed in metallic form, no statement about the speciation of Cd is possible: The detection limit of the microprobe would require a local enrichment of Cd by two to three orders of magnitude to get into a measurable range.

The residues of the Küpat VS process can be considered as an intermediate between conven-

tional bottom ash and the glasses produced in energy consuming high temperature processes (e.g. TRABER et al. 1999). They do not reach the degree of homogeneity of the latter by far, but an advantage is that the energy required for melting is derived solely from the waste itself. The advantages with respect to conventional bottom ash have already been discussed.

In several countries attempts have been made to guide the large material fluxes in today's waste management towards a re-use. They included not only the discussed glassy high temperature residues, but, e.g., also the use of bottom ash in road construction. Investigations for the use of municipal solid waste in the raw meal in concrete production are reported from Japan (SHIMODA et al. 2000). The Küpat residues have been tested for their potential to be used in cement or concrete (JACOBS, 1998). It was found that, from a technical point of view, the material cannot be used in the present form due to swelling processes (likely due to reactions of metallic Al with the alkaline pore fluids), although additional simple mechanical sorting of the residues prior to use had been carried out. Technical, ecological and regulatory aspects of the re-use of such residues have been discussed by TRABER et al. (2000).

The material characterisation showed that the Küpat residues have advantageous properties, which are believed to limit leaching of heavy metals in the long term. Life cycle assessments showed the importance of the recycling of residues (HELLWEG and HUNGERBÜHLER, 1999). Beyond the ecological aspects waste management is primarily an economic issue, and one may ask for the return of investment in the additional effort of high temperature slag treatment if the residues cannot be recycled. From this point of view, a minimum requirement would be the classification of the residues as so called "inert material", which would allow them to be landfilled at lower cost than conventional bottom ash. The Küpat residues pass the technical leaching test according to Swiss legislation (KÜNSTLER et al., 1994a), but the contents of Cu and Zn in the solid residues often exceed the limits that would allow them to be classified as "inert material". Hence, the present legislation provides no incentive for the further development and the application of such high temperature processes.

The present material characterisation provides a basis for the understanding of this leaching behaviour. Zn is almost completely bound to silicate phases, and Zn flux into solution is thus limited by the relatively small rates of silicate dissolution. On the other hand, Cu should be relatively readily available because large amounts of

this element are present in metallic form. The good performance of the residues with respect to Cu is therefore possibly the result of the physical-chemical conditions of the technical leaching test (e.g. $p(O_2)$) and possibly the enclosure of metal inclusions in the glass matrix.

5. Conclusions

Without use of additional energy, the high temperature process leads to increased melting, additional homogenisation, and a reduction of the specific surface area of residues. They have lower Cd, Pb, C and S contents than conventional MSWI residues, hence the danger of emissions of these elements from a potential landfill is lowered. An additional advantage shown in this study is, that Zn is incorporated into glassy or crystalline silicate phases.

Although these residues do not reach the quality obtained by other high-temperature processes, application of this process is believed to be a progress in waste management and appears to be particularly interesting at a time when economic arguments dominate.

The leaching behaviour of the material is expected to be a complex pattern resulting from interaction of the leaching solution with the various solid phases. This detailed material characterisation forms the basis for the interpretation of column leaching experiments and modelling of the long-term behaviour using computer codes for rock water interaction (TRABER, 2000).

References

BIOLLAZ, S., GROTEFELD, V. and KÜNSTLER, H. (1999): Separating heavy metals by the VS-process for municipal solid waste incineration. In: BARRAGE, A. and EDELMANN, X. (eds): R'99 Conference Proceedings, Geneva, vol. 2, 146–151.

BRANDL, H., HELLWEG, S., SCHMIDT, V., STUCKI, S. and WOCHELE, J. (eds) (1999): Forschung für eine nachhaltige Abfallwirtschaft. Ergebnisse des Integrierten Projekts Abfall im Schwerpunktprogramm Umwelt des Schweizerischen Nationalfonds 1996–1999. Paul Scherrer Institut, Villigen, 148 pp. (Abstracts available at www.IP-waste.unibe.ch).

DEER, W.A., HOWIE, R.A. and ZUSSMAN, J. (1962): Rock-Forming Minerals: Vol. 1 Ortho- and Ringsilicates. Longmans, London, 333 pp.

DEER, W.A., HOWIE, R.A. and ZUSSMAN, J. (1986): Melilite Group. In: Rock-Forming Minerals: Disilicates and Ring Silicates. Vol. 1B, 2nd ed., Longman, Harlow (Essex), 629 pp.

DEER, W.A., HOWIE, R.A. and ZUSSMAN, J. (1992): An Introduction to the Rock-Forming Minerals. 2nd ed., Longman, Harlow (Essex), 696 pp.

EISENHÜTTENLEUTE, VEREIN DEUTSCHER (ed.) (1995): Slag Atlas. Verlag Stahleisen, Düsseldorf, 616 pp.

GANGUIN, J. (1998): Kehrichtschlacke weist Reststoffqualität auf – Untersuchungen der chemischen Zusammensetzung und des Auslaugverhaltens von Kehrichtschlacke. Informationsbulletin des Amtes für Gewässerschutz und Abfallwirtschaft des Kantons Bern, 2/98, 40–47.

HELLWEG, S. and HUNGERBÜHLER, K. (1999): Wie die Modernisierung thermischer Entsorgungsverfahren zu Ökoverträglichkeit beiträgt. In: BRANDL, H., HELLWEG, S., SCHMIDT, V., STUCKI, S. and WOCHELE, J. (eds): Forschung für eine nachhaltige Abfallwirtschaft. Ergebnisse des Integrierten Projekts Abfall im Schwerpunktprogramm Umwelt des Schweizerischen Nationalfonds 1996–1999. Paul Scherrer Institut, Villigen. 37–46.

IBERG, R. (1971): Beitrag zu Thermochemie von Ziegeltonen. Tonindustrie Zeitung, 95 (3), 79–81.

JACOBS, F. (1998): Untersuchungen von Schlacken aus dem Küpat-Verfahren. TFB Wildegg (Technical Research and Consulting on Cement and Concrete), Report U973125, 12 pp.

JOHNSON, A. (1993): Chemische Eigenschaften und Langzeitverhalten der Müllschlacke. In: GAMPER, B. und BACCINI, P. (eds): Deponierung fester Rückstände aus der Abfallwirtschaft. vdf Hochschulverlag, ETH Zürich, 35–52.

KÜNSTLER, H., KLUKOWSKI, C. and GROTEFELD, V. (1994a): Der VS-Kombi-Reaktor der Firma Küpat AG. Müll und Abfall, Beiheft 31, 67–72.

KÜNSTLER, H., KLUKOWSKI, C. and GROTEFELD, V. (1994b): Der VS-Kombi-Reaktor zur Abfall- und Flugstaubschmelze. Abfall-Spektrum, 2/94, 17–19.

LEVIN, E.M., ROBBINS, C.R. and MCMURDIE, H.F. (1964): Phase Diagrams for Ceramists. The American Ceramic Society, Columbus, Ohio, 219 pp.

LEVIN, E.M., ROBBINS, C.R. and MCMURDIE, H.F. (1969): Phase Diagrams for Ceramists. 1969 supplement. The American Ceramic Society, Columbus, Ohio, 625 pp.

LICHTENSTEIGER, T. and ZELTNER, C. (1993): Wie lassen sich Feststoffqualitäten beurteilen? In: GAMPER, B. und BACCINI, P. (eds): Deponierung fester Rückstände aus der Abfallwirtschaft. vdf Hochschulverlag, ETH Zürich, 11–33.

SHAW, H.R. (1972): Viscosities of magmatic silicate liquids: an empirical method of prediction. Am. J. Sci., 272, 870–893.

SHIMODA, T., YOKOYAMA, S., and HIRAO, H. (2000): Eco-cement: A new Portland cement to solve municipal and industrial waste problems. Journal of Research of the Taiheiyo Cement Corporation, 138, 5–15.

STÄUBLI, B. (ed.) (1992): Emissionsabschätzung für Kehrichtschlacke. Bericht der Auftraggebergemeinschaft für das Projekt EKESA: AGW Kanton ZH und Abt. Umweltschutz Kanton AG. 156 pp.

TRABER, D., MÄDER, U., EGGENBERGER, U., SIMON, F.-G. and WIECKERT, C. (1999): Phase chemistry study of products from the vitrification processes AshArc and Deglor. Glastech. Ber. Glass Sci. Technol., 72(3), 91–98.

TRABER, D., JACOBS, F., MÄDER, U. and EGGENBERGER, U. (2000): Sekundärstoffe im Beton: Technische und ökologische Anforderungen. BFT: Betonwerk + Fertigteil-Technik (Concrete Plant + Precast Technology), 66(11), 76–84.

TRABER, D. (2000): Petrology, geochemistry and leaching behaviour of glassy residues of municipal solid waste incineration and their use as secondary raw material. PhD thesis, University of Bern, 197 pp.

TVA (1990): Technische Verordnung über Abfälle (SR 814.600). Schweizerischer Bundesrat. Eidg. Druck- und Materialzentrale, Bern, 32 pp. (http://www.admin.ch/ch/d/sr/c814_600.html)

WOCHELE, J., STUCKI, S., JAKOB, A. (1997): Earth's crust-quality residues from MSW incineration by improved thermal separation of heavy metals. In: BARRAGE, A. and EDELMANN, X. (eds): R'97 Conference Proceedings, Geneva, 5, 246–251

YODER, H.S.J. (1973): Melilite stability and paragenesis. Fortschr. Mineral., 50, 140–173.

ZELTNER, C. (1998): Petrologische Evaluation der thermischen Behandlung von Siedlungsabfällen über Schmelzprozesse. PhD thesis, ETH Zürich/EAWAG Dübendorf, Nr. 12688, 239 pp.

ZELTNER, C. and LICHTENSTEIGER, T. (2001): Thermal waste treatment and resource management – a petrologic approach to control the genesis of materials in smelting processes. Environmental Engineering and Policy. Springer-Verlag (Electronic Journal). See link at http://www.link.springer.de